Operational Optimization of the Lithium-Ion Batteries of TerraSAR-X/TanDEM-X

Fotios Stathopoulos, Kay Müller, Miguel Lino, Thomas Kraus, Patrick Klenk, and Ulrich Steinbrecher

***Abstract*—After a decade of successful TanDEM-X mission operations, the degradation of the satellite's battery capacity due to ageing has defined a new challenge for DLRs mission operations team. In response, a novel machine learning strategy has been gradually deployed in the Mission Planning System in order to optimize the battery utilization. The objective of this strategy is twofold: 1) protecting the operational state of the battery while 2) maximizing the executed SAR acquisitions under newly introduced planning restrictions. The limits, resulting in the battery utilization optimization, have been communicated to the customers in a user-friendly way in order to assist their future planning, minimizing the number of not-executed requests due to the new energy and power constraints imposed by the joint TerraSAR-X/TanDEM-X Mission Planning System. In this article, we 1) detail the quantitative approach to model the satellites' battery behavior in comparison to the previously used physical models, 2) outline the process of the new machine learning model as implemented in the Mission Planning System, 3) present the operational results of the model in comparison to satellite telemetry, and 4) discuss the evolution of the machine learning model toward higher accuracy telemetry estimations.**

***Index Terms*—Lithium-ion battery, machine learning, TanDEM-X, TerraSAR-X.**

I. Introduction

THE satellite of the TerraSAR-X mission: TSX [1], [2], was launched from Baikonur in Kazakhstan on a Dnepr-1 launcher on June 15, 2007. Its identically constructed twin satellite: TDX, which is required by the bistatic mission TanDEM-X [3]–[6], launched on June 21, 2010 in the same way. Both spacecraft were assembled by Airbus Defence and Space in Friedrichshafen. Based on an elaborated synthetic aperture radar (hereinafter: SAR) system calibration scheme [7], [8] the two satellites have been supplying high-quality radar data for more than a decade [9] in order to serve the two main mission goals: 1) scientific observation of earth and the provisioning of remote-sensing data for the commercial market explored by Airbus Intelligence Services (TerraSAR-X mission) and 2) the provision of scientific bistatic acquisitions and the generation of a global digital elevation model (DEM) of earth's surface (TanDEM-X mission) [3], [4], [10].

The TerraSAR-X/TanDEM-X ground segment is composed of three major elements designed and operated by DLR in Oberpfaffenhofen: the Instrument Operation and Calibration Segment (IOCS) provided by the Microwaves and Radar Institute [11]; the Payload Ground Segment provided by the German Remote Sensing Data Center (DFD) and the Remote Sensing Technology Institute (IMF) [12], [13]; and the Mission Operations Segment provided by the German Space Operations Center (GSOC) [14].

The space segment comprises both satellites, flying in formation in a sun-synchronous dusk–dawn orbit with a revisit period of 11 days [15]. Whereas several different formations have been configured over the years, TSX and TDX have flown in the majority of time in a helix close formation where TSX flies the reference orbit and the distance between both spacecraft is in the order of 200–500 m [16], [17]. Such a formation requires an extended monitoring of the status of the spacecraft to avoid collision and mutual radar illumination but allows for a good interoperability and flexibility to adjust TDX depending on the varying needs for bistatic acquisitions [17].

Despite having been designed for only five years of nominal lifetime, the health condition of both satellites after currently more than 13 (TSX) and 10 (TDX) years in orbit continues to allow a near-full utilization of its resources for the TerraSAR-X and TanDEM-X missions [18], [19]. Due to the strategy described in this article of monitoring and adjusting the battery-usage limits, current battery-utilization constraints are still by far smaller in comparison to those imposed by the available ground station downlink time or the on-board memory of the satellites [20]. Nevertheless, with continuous ageing of the batteries, an ever better understanding of their behavior during mission operations is needed in order 1) to support maximum possible imaging capacity and 2) to define and justify required restrictions, preventing overly low-voltage drops, which could threaten the spacecraft's health. The knowledge gained over more than a decade of operating successfully the two spacecraft has now enabled the implementation of a novel battery model with the aim of guaranteeing efficient operation of both the TanDEM-X and TerraSAR-X missions in the foreseeable future.

Manuscript received September 30, 2020; revised December 23, 2020 and January 14, 2021; accepted January 15, 2021. Date of publication February 11, 2021; date of current version March 25, 2021. The work was supported in part by the Deutsches Zentrum für Luft- und Raumfahrt e.V. (DLR) Institut für Raumflugbetrieb. *(Corresponding author: Fotios Stathopoulos.)*

Fotios Stathopoulos is with the German Space Operations Center (GSOC), German Aerospace Center (DLR), 82234 Wessling, Germany, and also with the Electrical and Computer Engineering School (ECE), National Technical University of Athens (NTUA), 15780 Athens, Greece (e-mail: fotios.stathopoulos@dlr.de, fstatho@mobile.ntua.gr).

Kay Müller and Miguel Lino are with the German Space Operations Center (GSOC), German Aerospace Center (DLR), 82234 Wessling, Germany (e-mail: kay.mueller@dlr.de; miguel.lino@dlr.de).

Thomas Kraus, Patrick Klenk, and Ulrich Steinbrecher are with the Microwaves and Radar Institute (HR), German Aerospace Center (DLR), 82234 Wessling, Germany (e-mail: t.kraus@dlr.de; patrick.klenk@dlr.de; ulrich.steinbrecher@dlr.de).

Digital Object Identifier 10.1109/JSTARS.2021.3056174

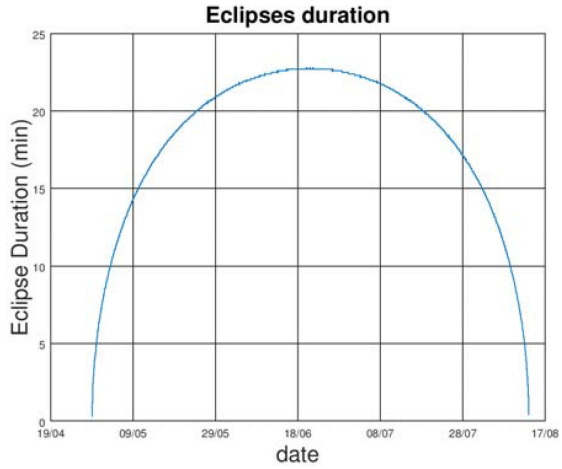

Fig. 1. Duration of the eclipses of TSX and TDX per orbit versus the DOY. The eclipses season starts on April 29th and last until August 14th every year. The maximum duration of 23 min is reached around the summer solstice (June 21st), where the solar panels are not facing the sun for about 24% of the orbit.

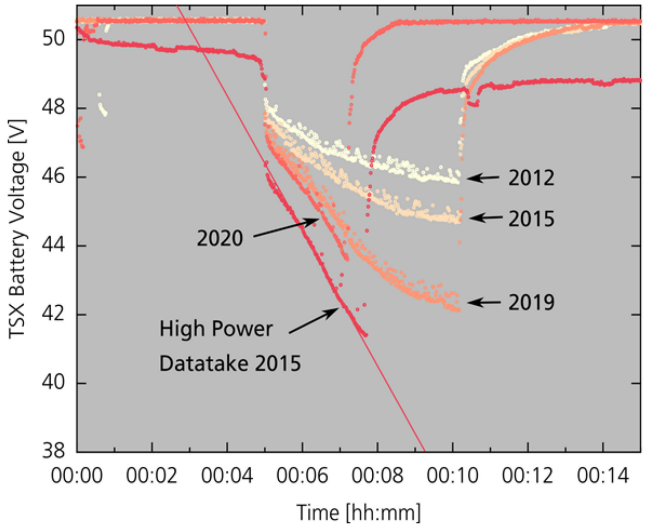

Fig. 2. Comparison of reference SAR acquisitions from 2012, 2015, and 2019. As of writing this article, the acquisition for 2020 has not been performed, but an acquisition of a similar type (but shorter duration) is shown. Note the linear character of the voltage decrease and the comparable lack of variation of the values for the high power datatake in 2015. This acquisition was the one that first raised awareness of the diffusion rate limitation present in the battery from that point onward.

In this article, after a brief introduction to the power system of the TSX and TDX satellites in Section II, the battery model will be described in detail while presenting its development process step by step (see Section III), followed by the evaluation of the operational results (see Section IV). Finally, the advantages of this quantitative approach are discussed while giving an outlook with respect to future improvements of the algorithm (see Section V).

II. Overview of the TSX/TDX Power Subsystem

TerraSAR-X and TanDEM-X's electrical power systems share the same design. Their power usage is roughly a factor of 10 higher during data acquisition than during nominal bus operations. This resulted in a design combining a lithium-Ion battery connected to a solar array, and a dusk–dawn orbit that allows for solar irradiation during all orbital revolutions (hereinafter called the sun phases), except for those between late April and mid-August during which the solar panel of the satellites are temporarily (part of the orbit) in the shadow of the earth (hereinafter called the eclipse phases). The duration of eclipses within one orbit depending on the day of year (DOY) is shown in Fig. 1.

For every SAR acquisition in the sun phases, the battery provides about three quarters of the consumed energy. The choice of orbit is, therefore, an important mission design element because it allows the battery to be recharged immediately afterward, unless the satellite is in eclipse. The charging process is controlled by maximum power point trackers (MPPT) implemented in hardware, which operate the solar array at its maximum output power until the battery voltage reaches 50.4 V. Then, the charge current is reduced while keeping the voltage constant until the battery is fully charged.

The battery consists of individual lithium-ion cells in three modules. Compared to the older nickel–hydrogen chemistry with its significantly larger cells, the failure of a single cell has much less impact on the provided power [21]–[24]. The solar generator likewise consists of several solar cells strings arranged in two panels. The power output of each panel is controlled by three MPPTs, with a two out of three redundancy. The instrument is directly connected to the unregulated voltage bus. As a result, its voltage varies between 50.4 V and a lower limit of 38 V during nominal operations, which is required by the input converter of the instrument.

In order to assess the battery's performance over the mission duration, a reference SAR acquisition is performed every year after the eclipse season (see Fig. 1) with the same settings and duration to ease the comparison between the years. Fig. 2 shows the voltage behavior for several of these yearly reference acquisitions. They represent a typical behavior of the discharge of a lithium-ion battery with an overall mathematically convex shape (which would turn linear and finally drop off quickly for longer discharges not employed on either satellite). With increasing degradation, the initial voltage drop at the start of the acquisition becomes larger and is used to assess the internal resistance of the battery. Also, the gradient of the voltage decrease during discharge becomes steeper over the years, resulting in lower voltages being reached faster when actively acquiring SAR data.

During the eclipse period of 2015, it was first noted that the behavior of the battery on TSX deviated from that of previous years. Instead of having a convex shape, the voltage dropped linearly from the beginning and with a larger gradient than expected, as for the "High-Power Datatake 2015" in Fig. 2. The variation of the measured data points was also noticeably smaller than before. An investigation by Airbus established that this new behavior was due to a diffusion rate limitation, i.e., the ability of the ions taking part in the battery's chemical reaction to diffuse to the surface of the electrodes was reduced when a high discharge current was applied. This lowered the apparent capacity of the battery.

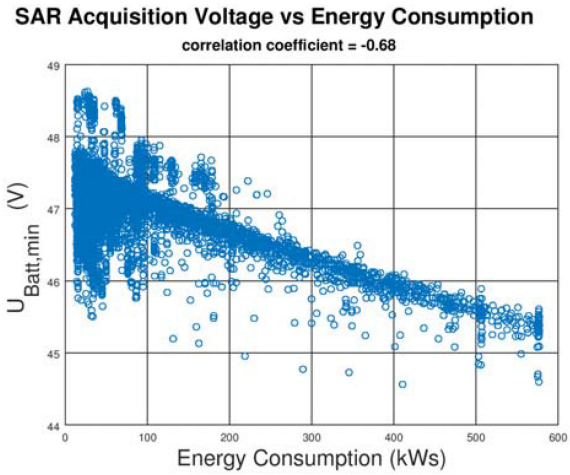

Fig. 3. Minimum voltage per SAR acquisition in the sun versus the energy consumption of the complete acquisition on the TDX satellite. The correlation coefficient is −0.68.

Failure detection of the battery is implemented in the FDIR concept of the satellites by switching OFF at first the instrument and eventually the bus components when a voltage of 38 V and lower is detected. This is called "disconnect of nonessential loads." Such an occurrence—although important to protect the battery and the satellite in general—would prevent planned SAR acquisitions from being executed (since the instrument is switched OFF) and requires extensive work from the operations team to assess the situation and to bring the satellite back into an operational state.

Several power and thermal constraints are considered in the Mission Planning System as described in [25] and [26]. The process of planning the acquisitions, therefore, needs to determine how many and what kind (e.g., in terms of SAR parameters such as the transmit duty cycle) of SAR acquisitions can be planned with a certain duration in a predefined time period while considering both previous acquisitions and the state of the battery.

Prior to reaching such low voltage values in the telemetry, a telemetry warning low-threshold will be triggered when falling below 42.5 V. This is, therefore, the threshold considered by the model for the analysis in the following section(s).

III. Method—The Chain Model

Traditionally, most of the battery management strategies applied for satellite missions, either for GSOC in-house operated satellites [22]–[24], [27] or for satellite missions of other mission operation centers [28], have been mainly based on the chemical composition of the satellite batteries and their internal physical properties. Such an approach typically suffices for safe mission operations during the nominal lifetime of a satellite while the batteries can be assumed to operate within their design limits, as it was the case in the first years of the TerraSAR-X and TanDEM-X mission. However, for a spacecraft operated far beyond its design lifetime, more sophisticated approaches are needed to guarantee efficient mission operations while preserving the health of the battery and the spacecraft in general.

After the first low-voltage events in 2015, we observed that the on-board mechanisms, using voltage telemetry parameters, and the existing algorithm in the mission planning system that modeled the calibrated energy consumption of the battery, were no longer in sync. In 2017, we performed a correlation analysis on the telemetry data of TSX and TDX comparing and combining it with the same dataset of mission planning so that the drop of the voltage could be simulated using the data available in mission planning. For the first time, we performed a data-driven analysis, combining telemetry data (the battery voltage at the end of a SAR acquisition) with the related data from the mission planning data pools (all data related to that SAR acquisition). The promising initial results of this statistical approach led to its incorporation in the decision process of the TerraSAR-X/TanDEM-X Mission Planning System [25], [29]. The main characteristics of this approach will be discussed in the following paragraphs, showing the behavior of the main battery parameters in relation to the mission operations.

A. Consumed Energy Versus Battery Voltage Drop

The first stage of the analysis was performed in order to assess the correlation of the energy consumed during a SAR acquisition, provided by the mission planning data pools, with the battery voltage drop, provided by the telemetry data. The first results, as depicted in Fig. 3, show the trend between the minimum battery voltage and the corresponding SAR acquisition's energy consumption. Note that the correlation coefficient of −0.68 seems rather low, which is mainly caused by a significant number of outliers, mostly below the dominating trend. Checking case by case the outliers of this analysis, especially the ones of higher energy consumption, we observed that they are related to SAR acquisitions close to previously executed ones where the time in between was insufficient to fully recharge the battery. In order to cope with this behavior, the "chain model" was defined: When two acquisitions are executed close enough to each other that the battery voltage does not raise back to the nominal range (∼50 V) after the execution of the previous one, they are considered by the model as one single acquisition with its duration being the sum of the durations.

With the aim of quantifying how close two acquisitions should be, in order to belong in the same chain, we repeated the analysis of the consumed energy of SAR acquisition chains versus the respective voltage at the end of the chain, considering several maximum distances between two consecutive acquisitions defining a chain (from 10 to 100 s). The highest correlation coefficient of −0.86 was found for chains of 60 s maximum separation between the two acquisitions, as shown in Fig. 4. This is the minimum separation between two consecutive SAR acquisitions to consider them in a separate chain.

B. Energy Versus SAR Acquisition Duration

A second parameter of interest is the SAR data acquisition duration. The high correlation between the total energy consumed during a SAR data acquisition and its execution duration, as depicted in Fig. 5, provides the opportunity to express any upper threshold on the energy provided by the battery in terms of SAR

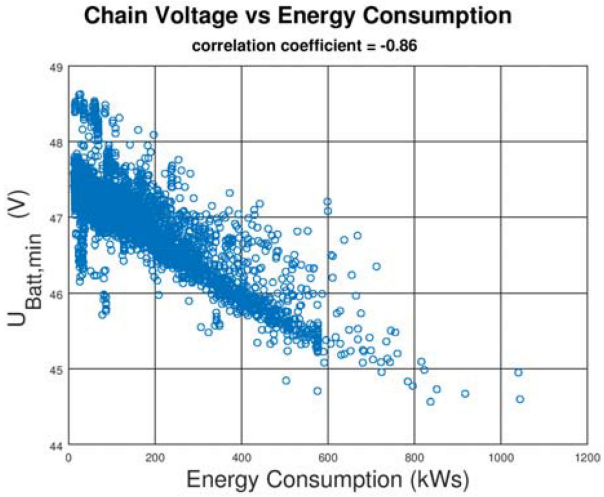

Fig. 4. Minimum voltage per SAR acquisition in the sun versus the energy consumption per chain of acquisitions on TDX satellite. The correlation coefficient is −0.86.

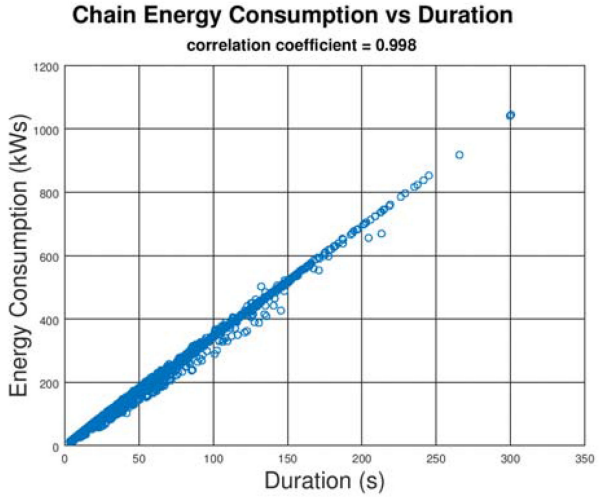

Fig. 5. Energy consumption in the sun versus the duration of individual SAR acquisitions on TDX satellite. The correlation coefficient is −0.998.

acquisition duration: The longer an acquisition lasts, the more energy is consumed.

C. SAR Acquisition Duration Versus Voltage Drop

Combining the previous two steps of the analysis provides the effect of a SAR data acquisition on the battery voltage drop depending on its duration: The longer a data acquisition, the lower the battery voltage drops.

Conversely, setting a limit on the maximum length a SAR acquisition directly restricts the battery minimum voltage reached during data acquisition. Based on the results of Fig. 6, the expected battery voltage drop can be controlled via imposing restrictions on the duration of the SAR acquisitions, either on a single one or in a chain. In mission operations terms, enforcing such a rather simple limit on the maximum duration of an acquisition has the advantage of enabling the communication

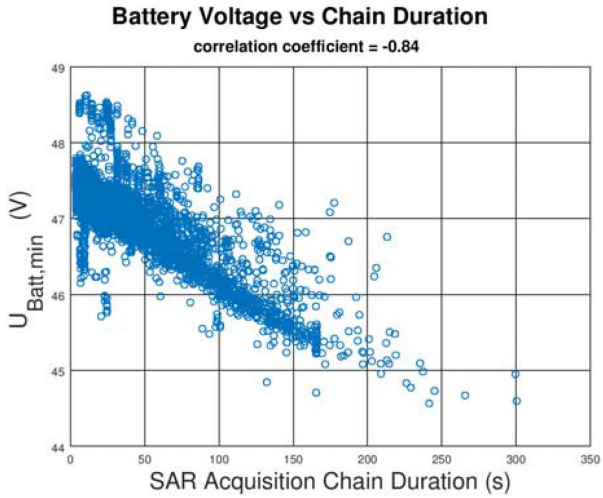

Fig. 6. Minimum voltage at the end of a SAR acquisition chain in the sun versus the sum of acquisition duration inside the chain on TDX satellite. The correlation coefficient is −0.84. Maximum separation between two consecutive acquisitions in order to be considered in the same chain is 60 s.

TABLE I
UPPER LIMITS OF TOTAL SAR ACQUISITION DURATION IN A CHAIN

	Sun Phases		Eclipse Phases	
Year	TSX	TDX	TSX	TDX
2017	-	-	-	165s
2018	200s	-	65s	165s
2019	170s	360s	65s	100s
2020	140s	330s	50s	90s

The thresholds of the chain model, as it has been applied on both TSX and TDX satellites since 2017, inside the Mission Planning System for both eclipses and sun phases.

of limits transparently to the users, aiding them in conveniently planning their acquisition strategy.

D. Long-Term Estimation of the Model-Based Limits

Based on the promising results presented in the previous sections, corresponding model-based SAR acquisition duration limits can be implemented in the mission planning system for the TerraSAR-X mission. The applied acquisition duration limits can be derived by the performance of the battery. The battery performance can be expressed based on the minimum voltage observed. For a longer period of past telemetry data, we create time series of the voltage level for dedicated SAR acquisition durations. The study has been initiated in 2017 [30]. Based on this analysis, the chain model has been operationally applied, as shown in Table I. Note that, being already in the eclipses phase of 2017, only the most recent TDX telemetry data (of that year's eclipse period) were considered to derive these limits at that time.

In 2018, it was required for the first time to perform a projection of the battery performance for the future, based on the performance knowledge gained during the previous year.

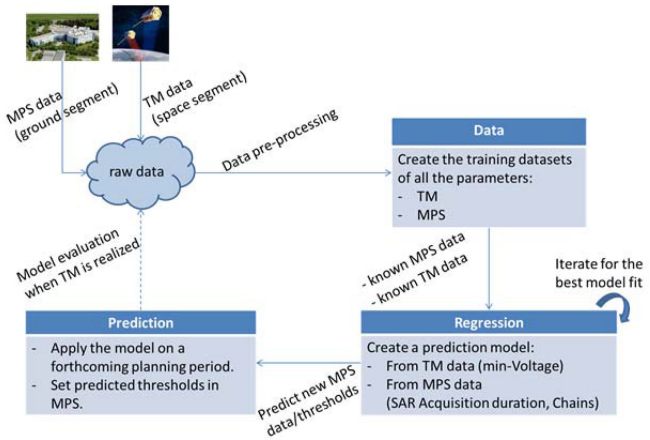

Fig. 7. Block diagram of the machine learning model applied in the Mission Planning System on the batteries of TSX and TDX satellites.

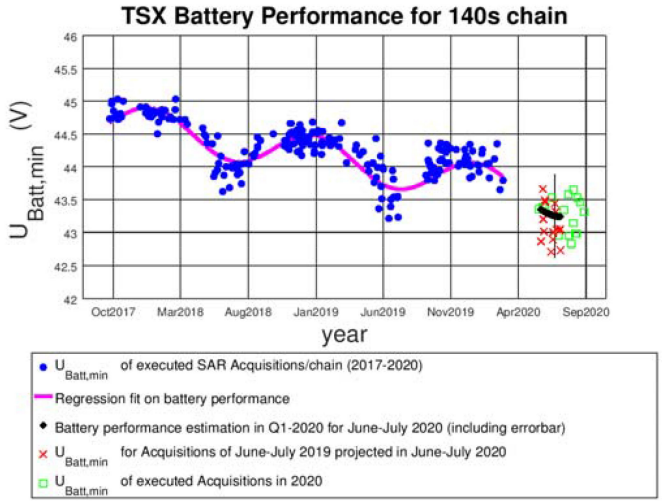

Fig. 8. TSX battery performance for chains of SAR acquisitions in the sun with a total duration of 140 s. Blue bullets show the minimum battery voltage according to satellite telemetry, whereas the magenta line is the regression fit. The estimated fit is plotted by the black rhombus, whereas with red points (x) are estimated minimum voltage values for the critical period of 2020 around the summer solstice derived according to the model in the first quarter of 2020. The measured minimum voltage of those SAR acquisitions/chains executed around the summer solstice of 2020 on TSX satellite are depicted by the green "square" boxes. The performance of the battery has been estimated quite closely to the actual telemetry when realized.

Therefore, an investigation into the long-term estimation of the corresponding thresholds was initiated, which we will detail in the following. Combining the data from the Mission Planning System (i.e., the ground segment) and the satellite telemetry (i.e., the space segment), we developed the first machine learning model for the batteries of TSX and TDX, as presented in Fig. 7, in order to estimate the performance of their respective batteries in the forthcoming mission periods and to be able to set the respective data acquisition duration thresholds in the Mission Planning System accordingly, several weeks/months in advance.

Thenceforth, every year the projection of the battery performance is based on past telemetry data available at that time. First, the information of the satellite telemetry (observed battery voltage) is matched to the information provided by the Mission Planning System (corresponding SAR acquisition properties), as shown in the upper left part of Fig. 7. Next, in the preprocessing step, we group the acquisitions to chains wherever the 60-s criterion discussed in the previous section was fulfilled, creating the dataset for the supervised learning analysis. Then, the regression analysis is performed, iterating several algorithms, in order to forecast the future performance of the satellite's battery during SAR acquisitions by the prediction model, shown in the lower right part of Fig. 7. Our target is to determine months in advance; the necessary limits of the chain model to be set in the Mission Planning System based on the battery voltage threshold we consider.

Over the years since 2018, we have considered several versions of linear regression functions applied in the machine learning logic presented in Fig. 7. As an example, we present here the analysis performed in the beginning of 2020 for the estimation of the data acquisition duration limit for TSX in the sun phases (as defined in Section II) in that year. However, the principle is the same for both cases, the acquisitions in sun and eclipse phases. First, we define a linear regression function in order to estimate the future performance of the battery voltage level, of each satellite, either in the sun or in the eclipse phases. Based on this expected performance, we derive corresponding data acquisition duration limits, which are then implemented in the Mission Planning System and communicated to the users.

Processing the telemetry of the past years, e.g., since 2017, it can be noticed that the yearly battery performance shows a clear seasonal trend, reaching minimum battery voltages every year around the summer solstice (as shown in Fig. 8). The observed battery behavior implies that the performance of the battery over the years can be modeled by an additive decomposition time series, $\mathrm{Y_t}$ [31]

$$Y_t = T_t + S_t + \varepsilon_t \tag{1}$$

where T_t is a trend, S_t is a seasonal component, and ε_t is an error term. In our case, as can be seen from the blue dots in Fig. 8, the seasonal component represents the yearly seasonality of sunlight illumination due to the satellite's orbit, with a minimum at the summer solstice, whereas the downward trend can be interpreted as the linear ageing of the batteries. Both parameters are related to time, which is the mission time (t_i) at any SAR acquisition. Based on these realizations, the regression function can be formulated as follows:

$$\mathrm{BattV_{est}}\ (i) = \alpha_0 + \alpha_1 \cdot t_i + \alpha_2 \cdot \sin\left(\frac{2\pi \cdot t_i}{12} - \varphi\right) + \varepsilon_i \tag{2}$$

where t_i is the execution time of a SAR acquisition (i), expressed in months but with resolution in seconds, and φ is the phase difference of the seasonality within a year (12 months). Since the phase difference is stable over time, we can incorporate it in the constant factor (α_0) of the regression function, which now becomes a multiple regression function of different time-related

factors

$$\mathrm{BattV}_{\mathrm{est}}\ (i) = \alpha_0 + \alpha_1 \cdot t_i + \alpha_2 \cdot \sin\left(\frac{2\pi \cdot t_i}{12}\right) + \alpha_3 \cdot \cos\left(\frac{2\pi \cdot t_i}{12}\right) + \varepsilon_i. \quad (3)$$

The model now is continuously adapted and validated based on the latest processed telemetry processed daily, extending the training period of the model as much as possible when the analysis is performed. In comparison, when this analysis was performed for the first time in 2018, the model has been initially trained and validated on past telemetry data of the last year (2017), and later it has been validated operationally. Nowadays, since the model is already operational, instead of separating the past data into a training and a validation period, we consider all observed data as a training dataset, while we validate the model by monitoring offline the performance of the model for several weeks with the new telemetry, prior to the official announcement and update of the model parameters. For the exemplary case discussed here, the training period of the model consisted of the chains of datatakes with a certain datatake duration, which have been acquired between the third quarter of 2017 and the first quarter of 2020 (depicted in Fig. 8 by the blue dots). For predicting the new limits on allowable data acquisition length based on the trained model, we focused on the period during which the battery performance estimation is most critical in the following year, which is the eclipse period (i.e., the months that the eclipses take place) in the months June and July 2020. Assuming a similar data acquisition load as in previous years, we used SAR acquisition chains executed in the same period in 2019, shifting their execution time by one year to 2020, as a dataset for applying the regression function defined earlier. We repeated the same analysis for several clusters of acquisition chains ((*0–10* s], (*10–20* s], etc.), each yielding different factors in the regression function. When applied to the dataset, the last cluster for which the estimation remains above the voltage threshold (here: 42.5 V, as in the telemetry monitoring system of the satellites), considering also the estimation error margins, defines the maximum duration of datatakes allowed to be planned.

Once the model is validated by new telemetry data (e.g., in 2020, this analysis was performed at the end of the first quarter of the year), the new limits to the acquisition duration is announced to the users. Note that the offline validation occurs prior to the critical period of the eclipses. While the estimations during the model validation are accurate, we assume (and it is later proven operationally), that the estimations in the critical period will be the same accurate.

Based on the concept described in Fig. 7, different versions of a linear regression algorithm can be considered for both the sun phases or the eclipse phases, on both satellites, including additional parameters from the Mission Planning System, such as the energy and power consumption during an acquisition, the attitude of the satellite at the time of the acquisition changing the solar panel illumination incidence angle, therefore, affecting the battery energy input, as well as the SAR acquisition duration, performing several iterations. Nevertheless, the machine learning concept via a linear regression algorithm is the driver of this analysis. This has been the first approach of a supervised learning algorithm, combining parameters by the Mission Planning System and the telemetry for the TSX and TDX battery voltage estimation.

After the model became operational, the battery performance is monitored on a daily basis by processing the telemetry arriving on the ground. The new data are fed back in the data pools of the model, 1) evaluating the performance of the battery and the efficiency of the model, while 2) updating the training datasets of the model with more recent data. This is the last step in the machine learning logic of this supervised learning model, presented in the bottom-left side of Fig. 7.

In summary, in this section, we detailed the SAR acquisition chain model, which, based on a machine learning algorithm, allows us to define the SAR acquisition limits on the chain model several weeks/months in advance. As an example, we described in detail the regression model applied on TSX for acquisitions executed in the sun phases for 2020. The same approach is applied for acquisitions executed on TSX in eclipses, as well as on TDX on both periods (sun phases or eclipses). Detailed operational results for all these cases are presented in Section IV.

IV. Results of the Chain-Model Implementation in the Mission Planning System

The implementation of the chain model in the Mission Planning System serves two use cases: 1) defining chain-model-based data acquisition duration limits during the sun phases, when a portion of the energy is provided by the solar panels, and 2) estimating corresponding limits for the eclipse periods, when exclusively the batteries provide the energy to the satellite. As a central result, we present the upper duration limits of data acquisition chains as evaluated based on our model and announced to the users since 2017 for all possible cases in Table I. Throughout the years, more knowledge and experience has been gained, minimizing the margins on the voltage threshold we have been considering.

A. Chain Model in the Sun Phases

In 2018, a low-voltage warning after a SAR acquisition in the sun phase was raised for the first time on TSX. This led to the decision to impose chain model based data acquisition duration limits for the sun-illumination periods. Since then, the performance of the batteries on both satellites has been closely and continuously monitored.

Due to the fact that the yearly minimum performance of the batteries occurs during the eclipse period, we decided to update the threshold of the chain model for the sun phases always before the start of the eclipses period, i.e., in early April every year, together with the update of the threshold for the eclipses. After the thresholds are communicated to the users, there is hardly any single SAR acquisition being ordered, which exceeds the duration limits. As a result, with the limits known to the users, very few acquisitions get rejected by the corresponding mission planning rule limit, most of which are part of a chain with another acquisition. On average, less than 1% of all the acquisitions considered by the mission planning algorithm are getting rejected

TABLE II
RESULTS OF REGRESSION ANALYSIS AS IN (3), FOR TSX IN 2020

parameters	140s	150s
α_0	45.05	44.94
α_1	-4.1E-05	-3.8E-05
α_2	-0.02	-7.60E-03
α_3	0.27	0.28
R^2	0.73	0.70
SD	0.21	0.24
mean estimation (V)	43.27	43.19
min estimation (V)	42.64	42.46

The results of the regression analysis for TSX satellite in 2020, defining the forecast of the chain model threshold to 140 s. Below the values of the model parameters are presented the coefficient of determination (R^2) as well as the standard deviation (SD), together with the mean voltage estimation value as well as the lowest voltage value expected, based on which we make the decision on the acquisition duration limit.

by the planning rule of the chain model. With respect to the observed battery voltage values, very few low-voltage warnings have been raised in the telemetry after we have been applying the chain-model-based limits in the sun phases in 2018 (single-digit number of cases yearly).

The results of the regression analysis for 2020, which has been detailed in the previous section, are presented in Table II, where we see the regression analysis allowing data acquisition chains of 140-s chains predicts minimum battery voltage values higher than 42.5 V, while allowing for 150-s duration might end up below the voltage threshold. Focusing on the worst case scenario, we, therefore, set the limit of acquisition duration in the sun phases of TSX to 140 s, as shown in Table I.

In Fig. 8, we present the operational results of all SAR Acquisitions with duration (130–140 s] for the period June–July 2020 on TSX as the green "square boxes," together with the estimation performed on January 2020, showing that the estimations are at the same level as the actual results. Similar results are observed on the TDX satellite.

B. Chain Model in the Eclipse Phases

The first low-voltage events were noticed during the eclipse period of 2015 when the power and energy demand from the battery were higher [30]. The chain model in the Mission Planning System was implemented in 2017 and has been operational since then. Due to the specific formation of the two satellites, in combination with the geographic location of the eclipses over the South Pole, the model was necessary to be operational in 2017 mainly on the TDX satellite. The exclusion zones [32] of TSX were overlapping with the eclipse areas of its orbit. Therefore, the latter satellite was prohibited from active SAR acquisitions during eclipse phases in any case. The second reversal of TanDEM's relative motion in the end of 2017 to balance the usage of on-board consumables (after the first one in 2013 [33]) made it, however, indispensable to apply the same model also for TSX thereafter. That was the first time that the SAR acquisition duration limits estimated based on the model has been set months in advance of the eclipse phase starting in April 2018. The model was validated by past telemetry data, becoming operational for the first time. After the first executed acquisitions in eclipse, we confirmed the calculations of the limits while we continued monitoring the performance of the battery in the following months of the eclipse period. The same process has been applied in the following years until today.

As an example, in the eclipse phase of 2020 the estimation of the SAR acquisition duration limit has been calculated in January 2020 after having processed the data of 2019, via the machine learning process described in Section III-D. The threshold has been announced by the end of the first quarter of 2020, as presented in Table I. During the eclipse season of 2020, from late-April to mid-August, only one low-voltage warning in an eclipse was raised on TSX, for a SAR acquisition of 49.3-s duration (only 0.7s lower than the upper limit of 50 s, as in Table I) that led to a voltage of 42.37 V (only 0.13 V lower than the threshold of 42.5 V). Due to the fact that the duration limit has been communicated well in advance to the users, there was no acquisition ordered inside an eclipse that exceeded the duration limit for TSX. Similarly for TDX, all SAR acquisition requests were well below the announced data acquisition duration limit; therefore, no low-voltage warning was raised. In this way, we succeeded to allow, every year since 2017, the maximum duration of acquisitions during eclipses while keeping the voltage higher than the telemetry warning threshold values.

V. FURTHER DEVELOPMENT

In this article, we have presented the process of modeling the battery voltage based on the duration of SAR acquisitions within a chain. This can be considered as a single independent variable regression model.

In parallel, in a two-step process, we regress and estimate, in the long term, the battery performance for specific duration-cluster chains, allowing us to define in advance the acquisition duration limits in order to respect the voltage thresholds for forthcoming periods, and announce them to the users.

As an evolution of this concept, we are developing a multiple linear regression model, considering more parameters already available in the Mission Planning System, including the mission time, as independent variables of a linear regression algorithm. Our intention is to increase the accuracy of the voltage estimation on every single SAR acquisition. For the time being this model is under evaluation in the Mission Planning System, it is running in the background of the planning algorithm, making all the calculations, but without taking any operational decisions.

Furthermore, under this machine learning modeling concept, we gradually develop and apply operationally the "telemetry prediction while planning" concept, combining information by the space segment (the telemetry datasets) and the ground segment (the Mission Planning datasets). Under this rationale, any telemetry parameter could replace the battery voltage as the dependent variable of the model, being able to forecast its performance while planning, setting new planning rules according to the estimations of the model, and finally optimizing the utilization of the available resources of this telemetry parameter within the Mission Planning System.

VI. Conclusion

More than 10 years of TDX operations and 13 of TSX compelled us to investigate novel approaches for the battery operations strategy. As detailed in this article, we defined the chain model, expressing the voltage drop through the acquisition duration, which apparently is the dominating factor for the voltage drop. The next step was to analyze the long-term performance of the acquisition chains. We managed to model their performance over time, and through a machine learning model, we estimate their performance in future periods. Based on the satellite orbit, we considered the worst case scenario, occurring around the summer solstice. As a result, we are able several months in advance to define an acquisition duration limit applied for the whole year, maximizing the battery utilization, while preserving the battery properties within the nominal telemetry ranges. This method has secured the battery operations on both satellites since 2017.

The data-driven approach on the battery strategy that we introduced can be further applied on any mission with similar variations on the power and energy demand, regardless of the chemical composition of the battery.

In parallel, via this machine learning concept, making decisions on forecasted telemetry data, we performed a first step toward applying artificial intelligence methods on the mission operations tools and the decision mechanisms of the Mission Planning System.

Acknowledgment

The authors would like to thank the TerraSAR-X/TanDEM-X operations team at the German Space Operations Center (GSOC), especially all the colleagues of the Power and Thermal team (PTS), the Mission Planning Operations team (MPS Ops), and the Mission Planning System Developers team (MPS DEV).

References

[1] R. Werninghaus and S. Buckreuss, "The TerraSAR-X mission and system design," *IEEE Trans. Geosci. Remote Sens.*, vol. 48, no. 2, pp. 606–614, Feb. 2010.

[2] S. Buckreuss, R. Werninghaus, and W. Pitz, "The German satellite mission TerraSAR-X," in *Proc. IEEE Radar Conf.*, 2008, pp. 1–5.

[3] G. Krieger *et al.*, "TanDEM-X: A satellite formation for high-resolution SAR interferometry," *IEEE Trans. Geosci. Remote Sens.*, vol. 45, no. 11, pp. 3317–3341, Nov. 2007.

[4] G. Krieger *et al.*, "TanDEM-X: A radar interferometer with two formation-flying satellites," *Acta Astronaut.*, vol. 89, pp. 83–98, 2013.

[5] G. Krieger *et al.*, "The TanDEM-X mission: Overview and status," in *Proc. IEEE Int. Geosci. Remote Sens. Symp.*, Jul. 2007, pp. 1–5.

[6] G. Krieger, M. Zink, D. Schulze, I. Hajnsek, and A. Moreira, "TanDEM-X: Mission overview and status," in *Proc. Int. Conf. Spacecraft Formation Flying Missions Technol.*, 2011, pp. 1–10.

[7] M. Schwerdt, B. Brautigam, M. Bachmann, B. Döring, D. Schrank, and J. H. Gonzalez, "Final TerraSAR-X calibration results based on novel efficient methods," *IEEE Trans. Geosci. Remote Sens.*, vol. 48, no. 2, pp. 677–689, Feb. 2010.

[8] M. Schwerdt *et al.*, "In-orbit calibration of the TanDEM-X system," in *Proc. IEEE Int. Geosci. Remote Sens. Symp.*, Jul. 2011, pp. 2420–2423.

[9] M. Schwerdt *et al.*, Radiometric performance of the TerraSAR-X mission over more than ten years of operation," *Remote Sens.*, vol. 10, no. 5, 2018, Art. no. 754.

[10] G. Krieger, H. Fiedler, I. Hajnsek, M. Eineder, M. Werner, and A. Moreira, "TanDEM-X: Mission concept and performance analysis," in *Proc. IEEE Int. Geosci. Remote Sens. Symp.*, Jul. 2005, pp. 4890–4893.

[11] U. Steinbrecher, D. Schulze, J. Boer, and J. Mittermayer, "TerraSAR-X instrument operations rooted in the system engineering and calibration project," *IEEE Trans. Geosci. Remote Sens.*, vol. 48, no. 2, pp. 633–641, Feb. 2010.

[12] S. Buckreuss and B. Schattler, "The TerraSAR-X ground segment," *IEEE Trans. Geosci. Remote Sens.*, vol. 48, no. 2, pp. 623–632, Feb. 2010.

[13] B. Schättler, M. Wolfmüller, R. Reißig, H. Damerow, H. Breit, and E. Diedrich, "A description of the data-driven SAR data workflow in the TerraSAR-X payload ground segment," in *Proc. Int. Geosci. Remote Sens. Symp.*, Sep. 2004, pp. 4543–4547.

[14] E. Maurer *et al.*, "TerraSAR-X Mission Planning System: Automated command generation for spacecraft operations," *IEEE Trans. Geosci. Remote Sens.*, vol. 48, no. 2, pp. 642–648, Feb. 2010.

[15] R. Kahle and S. D'Amico, "The TerraSAR-X precise orbit control—Concept and flight results," in *Proc. Int. Symp. Space Flight Dyn.*, May 2014. [Online]. Available: https://www.researchgate.net/publication/263200500_The_TerraSAR-X_Precise_Orbit_Control_-_Concept_and_Flight_Results

[16] S. D'Amico, O. Montenbruck, C. Arbinger, and H. Fiedler, "Formation flying concept for close remote sensing satellites," in *Proc. 15th AAS/AIAA Space Flight Mechanics Conf.*, Jan. 2005, pp. 831–848.

[17] R. Kahle, B. Schlepp, S. Aida, M. Kirschner, and M. Wermuth, "Flight dynamics operations of the Tandem-X formation," in *Proc. 12th Int. Conf. Space Operations*, Jun. 2012, pp. 891–902.

[18] A. Moreira *et al.*, "TanDEM-X: A TerraSAR-X add-on satellite for single-pass SAR interferometry," in *Proc. Geosci. Remote Sens. Symp.*, Sep. 2004, pp. 1000–1003.

[19] A. Bojarski *et al.*, "TanDEM-X long-term system performance after 10 years of operation," *IEEE J. Sel. Topics Appl. Earth Observ. Remote Sens.*, to be published, doi: 10.1109/JSTARS.2021.3055546.

[20] F. Stathopoulos, G. Guillermin, C. G. Acero, K. Reich, and F. Mrowka, "Evolving the operations of the TerraSAR-X/TanDEM-X Mission Planning System during the TanDEM-X science phase," in *Proc. 14th Int. Conf. Space Operations*, May 2016, doi: 10.2514/6.2016-2571.

[21] J. Herman, A. Davis, K. B. Chin, M. Kinzler, S. Scholz, and M. Steinhoff, "Life with a weak heart," in *Proc. 12th Int. Conf. Space Operations*, Jun. 2012. [Online]. Available: https://elib.dlr.de/76288/

[22] K. Müller and A. K. Balan, "Battery operations for the TET–1 spacecraft," in *Proc. 13th Int. Conf. Space Operations*, May 2014, doi:10.2514/6.2014-1732.

[23] A. K. Balan and K. Müller, "Operational experience with nickel hydrogen and lithium-ion batteries," in *Proc. AIAA Space Astronaut. Forum Expo.*, Aug./Sep. 2015, doi:10.2514/6.2015-4659.

[24] K. Müller, S. Löw, J. Herman, R. Gaston, and A. Davis, "End-of-life power management on the grace satellites with several failed battery cells," in *Proc. 70th Int. Astronautical Congr.*, Oct. 2019. [Online]. Available: https://elib.dlr.de/129495/

[25] F. Mrowka *et al.*, "The joint TerraSAR-X/TanDEM-X Mission Planning System," in *Proc. IEEE Int. Geosci. Remote Sens. Symp.*, Jul. 2011, pp. 3971–3974.

[26] C. Lenzen, M. Wörle, F. Mrowka, M. Geyer, and R. Klaehn, "Automated scheduling for TerraSAR-X/TanDEM-X, " in *Proc. Int. Workshop Plan. Scheduling Space*, Jun. 2011. [Online]. Available: http://robotics.estec.esa.int/IWPSS/IWPSS_2011/Papers/Lenzen_Paper.pdf

[27] M. M. Witkowski, E. S. Davis, and R. W. Gaston, "GRACE - 15 Years of adapting to aging equipment," in *Proc. 15th Int. Conf. Space Operations*, 2018.

[28] T. Ormston *et al.*, "Lithium ion battery management strategies for European Space Operations Centre Missions," in *Proc. 13th Int. Conf. Space Operations*, May 2014.

[29] F. Mrowka, T. Göttfert, M. Wörle, B. Schättler, and F. Stathopoulos, "The TerraSAR-X/TanDEM-X Mission Planning System: Realizing new customer visions by applying new upgrade strategies," in *Proc. 14th Int. Conf. Space Operations*, May 2016.

[30] F. Stathopoulos, C. Lenzen, and F. Mrowka, "Adapting the battery model in the Mission Planning System of ageing satellites," in *Proc. 15th Int. Conf. Space Operations*, May/Jun. 2018.

[31] T. Hastie, R. Tibshirani, and J. Friedman, *The Elements of Statistical Learning*. Berlin, Germany: Springer, 2008.

[32] E. Maurer, S. Zimmermann, F. Mrowka, and H. Hofmann, "Dual satellite operations in close formation flight," in *Proc. 12th Int. Conf. Space Operations*, Jun. 2012.

[33] E. Maurer, R. Kahle, G. Morfill, B. Schlepp, and S. Zimmermann, "Reversal of TanDEM-X's relative motion from counter-clockwise to clockwise," in *Proc. 13th Int. Conf. Space Operations*, May 2014.